Compositional and structural analyses of the photosystem II isolated from the red alga *Cyanidioschyzon merolae*

Joanna Kargul[a], Marko Boehm[b], Nina Morgner[c], Carol V. Robinson[c], Peter J. Nixon[b], James Barber[a,*]

[a]Division of Molecular Biosciences, Faculty of Natural Sciences, Imperial College London, London, SW7 2AZ, UK
[b]Division of Biology, Faculty of Natural Sciences, Imperial College London, London, SW7 2AZ, UK
[c]Department of Chemistry, Physical and Theoretical Chemistry Laboratory, University of Oxford, Oxford OX1 3QZ, UK
[*]Corresponding author. Tel. No. +44 2075945266; Fax No. +44 2075945267; E-mail: j.barber@imperial.ac.uk

Abstract: Members of the rhodophytan order *Cyanidiales* are unique among phototrophs in their ability to live in extremely low pH levels and moderately high temperatures. The photosynthetic apparatus of the red alga *Cyanidioschyzon merolae* represents an intermediate type between cyanobacteria and higher plants, suggesting that this alga may provide the evolutionary link between prokaryotic and eukaryotic phototrophs. While red algal PSI resembles that of the higher plants, the PSII complex is more reminiscent of the cyanobacterial ancestor in that it contains phycobilisomes as the light-harvesting system instead of Chl*a*/*b* binding proteins of green algae and higher plants, as well as the PsbU and PsbV subunits stabilising the oxygen evolving complex (OEC). The most remarkable feature of the red algal PSII is the presence of the fourth extrinsic protein of 20 kDa (PsbQ′) which is not found in the cyanobacterial OEC and which is distantly related with the green algal PsbQ. This feature together with some differences in the structural cooperation between the OEC subunits suggests that the lumenal side of red algal PSII may vary from the prokaryotic ancestor. In order to elucidate the structural differences between cyanobacterial and eukaryotic PSII, we have isolated highly active and stable dimeric complexes of the *C. merolae* PSII and subjected them to high throughput crystallization and mass spectrometry analyses. Here we report the full subunit composition and preliminary results of 3D crystallization of the dimeric *C. merolae* PSII.

Keywords: PSII structure; *Cyanidioschyzon merolae*; X-ray diffraction; mass spectrometry

Introduction

Recently, the crystal structure of photosystem II (PSII) isolated from the thermophilic cyanobacterium *Thermosynechococcus vulcanus* has been reported at a resolution of 1.9 Å (Shen *et al*., submitted). This atomic structure has confirmed a working model for understanding the water splitting reaction based on the previous crystallographic structures of cyanobacterial PSII obtained in our laboratory (Ferreira *et al.*, 2004; Kargul *et al*., 2007; Murray *et al*., 2008a; Murray *et al*., 2008b) and others (Kamiya and Shen, 2003; Loll *et al*., 2005; Guskov *et al*., 2009; Yano *et al*., 2006). The catalytic site is composed of a Mn_4Ca-cluster surrounded by a number of highly conserved amino acids. Although the precise arrangement of the metal ions was uncertain in the available crystallographic structures of PSII (due to the resolution limitation and possible radiation modifiction during diffraction data collection), the model which places three Mn ions and a Ca ion at the corner of a cubane with oxo-bridges and the forth Mn linked to the cubane via a bridging oxygen has gained support in the latest atomic structure of PSII (Shen *et al*., submitted), as well as from quantum mechanical considerations (Sproviero *et al*., 2008, Dau *et al*., 2008; Siegbahn, 2009).

Although we now have a detailed structural model of PSII from cyanobacteria at an atomic resolution, no corresponding structure of the eukaryotic PSII complex has been reported to date. To this end, we isolated and characterized PSII from the extremophilic unicellular red alga *Cyanidioschyzon merolae* aiming at structural characterization of this eukaryotic PSII complex. *C. merolae* belongs to the rhodophytan order *Cyanidiales* whose members thrive in acidic hot springs (Ciniglia *et al*., 2004), and are unique among phototrophs in the ability to live in extremely low pH levels (pH 0.2-4) and moderately high temperatures (40-56ºC). Furthermore, *C. merolae* is considered to be one of the most primitive photosynthetic prototrophs because it diverged near the

root of the red algal lineage that forms a basal group within the photosynthetic eukaryotes (Nozaki *et al*., 2003). It is well established that the oxygen evolving complex (OEC) from *C. merolae* is stabilized by 4 extrinsic lumenal subunits: cyanobacterial-like PsbV and PsbU, the evolutionary conserved PsbO subunit, and an additional 20-kDa subunit PsbQ′ exhibiting low homology with the higher plant and green algal PsbQ polypeptides (Ohta *et al*., 2003). The precise localization of this subunit and its role in stabilization of the OEC are currently unknown, although low-resolution single particle analysis and reconstitution experiments suggested that red algal PsbQ′ directly binds to CP43 of the core complex independently of other extrinsic proteins and is required for effective binding of the PsbV and PsbU subunits (Gardian *et al*., 2007; Enami *et al*., 2008). In contrast, PsbQ in higher plants functionally associates with PSII via its direct interaction with both PsbO and PsbP (reviewed in Enami *et al*., 2008). Interestingly, PsbQ′ can functionally replace PsbQ in spinach during cross-reconstitution experiments despite their low amino acid sequence homology (Enami *et al*., 2008). Moreover, it has been shown that the binding mode of PsbV differs between cyanobacteria and red alga, in that the red algal PsbV binds via other extrinsic subunits, whereas its cyanobacterial counterpart binds directly with the PSII core (reviewed in Enami *et al*., 2008). All these observations point towards significant structural differences on the lumenal side of PSII at various evolutionary stages.

The logic of working with *C. merolae* was to obtain a crystal structure of a eukaryotic form of PSII using an organism which was likely to provide a very stable form of the enzyme. Here we describe the fist steps towards the ultimate goal of obtaining the first structure of eukaryotic PSII. We demonstrate that a highly active and robust preparation of the dimeric PSII from *C. merolae* can be used to obtain 3D crystals of this complex.

Materials and Methods

Functionally active Photosystem II (PSII) has been isolated from the red alga *Cyanidioschyzon merolae*, strain N1332 (obtained from the NIES microbial culture collection). Thylakoid membranes were prepared from late-log phase cells grown in the Allen 2 medium (OD_{682} 3.5), using a modified procedure of Adachi *et al*. (2009). The cells were collected by centrifugation at 4,000 x g, washed once with buffer A (40 mM MES-NaOH, pH 6.1, 25% (w/w) glycerol, 10 mM $CaCl_2$, 5 mM $MgCl_2$) and resuspended in buffer A supplemented with 50 µg/ml DNAse I and the Complete™ protease inhibitor cocktail (Roche Diagnostics GmbH). Cells were broken by passing through a French Press (≈ 2000 psi) twice. Thylakoids were pelleted by centrifugation at 104,200 x g for 30 minutes at 4°C and washed once with buffer A. The thylakoid pellets were resuspended in buffer A at a chlorophyll (Chl) concentration of 2-3 mg/ml, snap-frozen in liquid N_2 and stored at -70°C prior to use. The dimeric PSII has been isolated by two-step anion exchange chromatography according to the modified protocol of Adachi *et al*. (2009) using the DEAE ToyoPearl 650 M followed by DEAE ToyoPearl 650 S chromatographic media. Thylakoids (1 mg/ml Chl) were solubilised with 1.2% (w/v) dodecyl-β-D-maltoside (DDM, Biomol) by stirring in the dark at 4ºC for 40 min. Soluble fraction was collected by centrifugation at 100,000 g for 30 min, then loaded onto the DEAE ToyoPearl 650 M column equilibrated with buffer B (40 mM MES-NaOH, pH 6.1, 25% (w/w) glycerol, 3 mM $CaCl_2$, 0.03% (w/w) DDM). The immoblised crude PSII was washed with the wash buffer (40 mM MES-NaOH, pH 6.1, 25% (w/w) glycerol, 3 mM $CaCl_2$, 0.09 M NaCl, 0.03% (w/v) DDM), then eluted with Elution 1 buffer (40 mM MES-NaOH, pH 6.1, 25% (w/w) glycerol, 3 mM $CaCl_2$, 0.23 M NaCl, 0.03% (w/v) DDM), and dialysed against buffer A supplemented with 0.03% DDM overnight at 4ºC in the dark. Dialysed crude PSII was loaded onto the DEAE ToyoPearl 650 S column (equilibrated with buffer A + 0.03% (w/v) DDM) to separate the PSII monomers and dimers using a continuous gradient of 0.05-0.15 M NaCl. The PSII dimer fractions were pooled and concentrated using the VivaSpin-20 (Sartorius Stedim Biotech) concentrating devices to at least 3 mg/ml Chl. Functional activity of purified thylakoids and PSII dimers (5 µg Chl) was measured using a Clark-type electrode (Hansatech). Measurements were performed at 30ºC in buffer A in the presence of 0.125 mM 2,6-dichloro-*p*-benzoquinone (DCBQ) and 2.5 mM potassium ferricyanide as the exogenous electron acceptors, using white light illumination intensity of 6,000 µE. In addition, samples have been biochemically analysed by size exclusion chromatography, SDS-PAGE, and mass spectrometry, using standard procedures. The highly active and pure dimeric PSII was subjected to extensive 3D crystallisation trials using a Mosquito nano-litre high throughput robot (TTP Labtech) and 14 commercially available screens pre-dispensed into 96 well MRC plates.

Results and Discussion

We set out to purify a highly active, intact and homogenous preparation of the *C. merolae* dimeric PSII

that wocould be suitable for 3D crystallization trials. Following solubilisation of thylakoids with the detergent (dodecyl-β-D-maltoside, DDM) we separated PSII monomers and dimers using a 2-step anion exchange chromatography approach (see Figure 1). In the second step, we purified a robust and higly active PSII dimer

Table 1. LC/MS and MS/MS analysis of protein composition of the *C. merolae* dimeric PSII

Protein subunit	Calculated mass from database	No. of peptides	Experimental mass
PsbA	39706	3	39218
PsbB	56300	6	56218
PsbC	51912	7	50410
PsbD	39290	3	37910
PsbE	9094	2	9084
PsbF	4706	2	4504
PsbH	7220	3	6644
PsbI	4475	3	4473
PsbJ	3991	2	3865
PsbK	4895	2	4867
PsbL	4382	1	4298
PsbM	16126	3	16054
PsbN	4725	1	4688
PsbO	35454	12	34757
PsbQ′	23622	5	23504
PsbT	3791	2	3769
PsbU	16847	6	16673
PsbV	16609	2	16350
Psb28	12580	2	12466
PsbX	4592	1	4376
PsbY	3926	2	3921
ycf12	3792	1	3732
PsbZ	6484	1	6396
Psb27	22017	3	21845

preparation (yield 3.5%) that was stable for up to 24 hours of incubation at an ambient temperature (see Figure 2b). The homogeneity of the sample was verified by size-exclusion chromatography which showed a single elution peak with the retention time corresponding to the PSII dimer (data not shown). The oxygen evolving activity varied between 3200-4300 μmoles O_2/mg Chl/h for different preparations tested. It was the highest recorded oxygen evolving activity obtained under our experimental conditions, and exceeded the activity of PSII isolated from the thermophilic cyanobacterium *Thermosynechococcus elongatus* used to obtain the X-ray structure of PSII (Ferreira *et al*., 2004). Moreover, this preparation retained its oxygen evolving activity when illuminated with high light intensities (up to 13,000 μE, see Figure 2a), indicating that the oxygen evolving complex remained intact when subjected to a high light stress.

We analysed the subunit composition of the purified *C. merolae* PSII dimer by biochemical and mass spectromentry approaches. Table 1 and Figure 3a show that the reaction centre subunits (D1, D2), inner antenna subunits (CP43, CP47), four extrinsic subunits stabilizing the OEC (PsbO, PsbU, PsbV, PsbQ′), and small intrinsic subunits were present in our preparation. Interestingly, our mass spectrometry analysis showed the presence of the PSII auxiliary subunits Psb27 and Psb28 implied in the regulation of the PSII repair cycle and biogenesis (Nowaczyk *et al.*, 2006; Dobáková *et al*., 2009). However, their stoichiometry of binding to PSII is presently unknown.

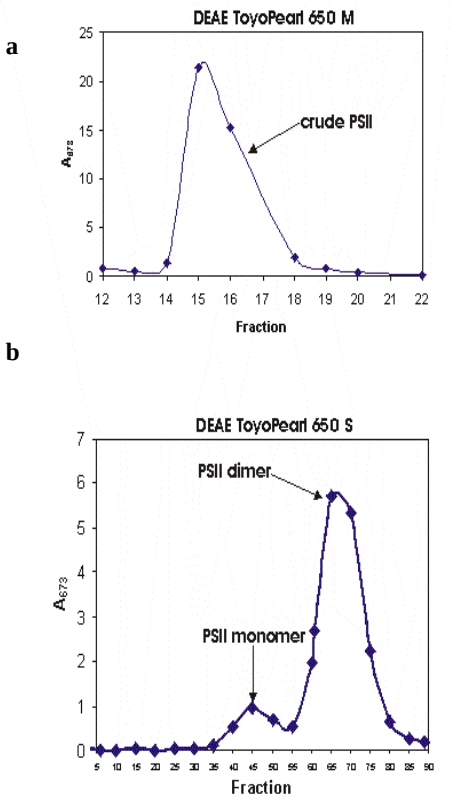

Figure 1. Purification of the *C. merolae* PSII. PSII was purified using two-step anion exchange chromatography. In the first step (a), crude PSII was purified which was subsequently separated into PSII monomer and dimer fractions (b).

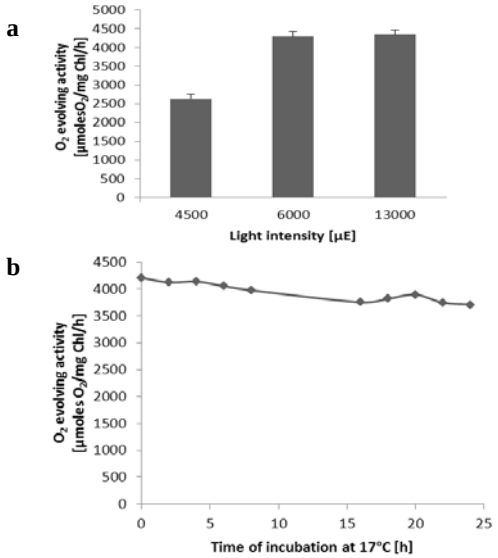

Figure 2. Stability of purified *C. merolae* PSII. Activity of PSII dimers was measured at various light intensities (a) or as a function of time over a 24-hour period of incubation at 17ºC in the dark (b). Oxygen evolving activity of PSII was measured at 30ºC in the presence of 0.125 mM DCBQ and 2.5 mM ferricyanide as the exogenous electron acceptors.

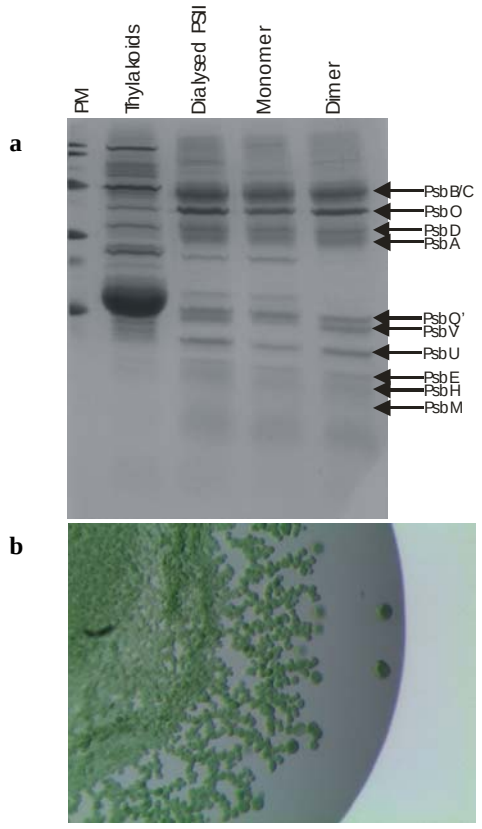

Figure 3. High-throughput screening of crystal-forming conditions using the *C. merolae* PSII dimer. (a) Sitting drops of 200 nl were set up at 4ºC or 20ºC by mixing a PSII dimer sample (1.4 mg Chl/ml) and mother liquor of 14 various crystallization screening kits (96 conditions per kit). (b) SDS-PAGE analysis of the *C. merolae* PSII dimer subunits. Proteins (5 ug Chl/lane) were separated on a 15% polyacrylamide gel, then visualized by Coomassie staining. PM, prestained marker. The PSII subunits are arrowed on the right-hand side of panel a.

Having obtained a highly robust and homogenous preparation of the *C. merolae* dimeric PSII we used it for extensive crystallization trials aiming at obtaining well-diffracting 3D crystals of this eukaryotic PSII. Initially, we tried to manually reproduce crystallization conditions that were successfully used to obtain crystals of PSII from *T. elongatus* (Ferreira *et al*., 2004) and a related red alga *Cyanidium caldarium* (Adachi *et al*., 2009). These conditions did not yield any crystals when the dimeric *C. merolae* PSII was used. To search for alternative conditions, we have performed high throughput robot-based screening using 14 commercially available crystallizations screens. In this approach, we identified 9 conditions which yielded 3D crystals (see Figure 3b) with some diffracting properties (data not shown). Work is under way to optimise these conditions in order to produce crystals with improved X-ray diffraction characteristics.

Acknowledgement

J.K, M.B, J.B. and P.N. acknowledge the support of EPSRC (grant EP/F00270X/1) to conduct this work.

References

Adachi H, Umena Y, Enami I, Henmi T, Kamiya N, Shen JR (2009) Towards structural elucidation of eukaryotic photosystem II: Purification, crystallization and preliminary X-ray diffraction analysis of photosystem II from a red alga. Biochim. Biophys. Acta 1787: 121-128.

Ciniglia C, Yoon HS, Pollio A, Pinto G, Bhattacharya D (2004) Hidden biodiversity of the extremophilic *Cyanidiales* red algae. Mol. Ecol. 13: 1827-1838.

Dau H, Grundmeier A, Loja P, Haumann M (2008) On the structure of the manganese complex of photosystem II: extended-range EXAFS data and specific atomic-resolution models for four S-states. Philos Trans R Soc Lond B Biol Sci. 363: 1237-1243

Dobáková M, Sobotka R, Tichý M, Komenda J (2009) Psb28 protein is involved in the biogenesis of the photosystem II inner antenna CP47 (PsbB) in the

cyanobacterium *Synechocystis* sp. PCC 6803. Plant Physiol. 149: 1076-1086

Enami I, Okumura A, Nagao R, Suzuki T, Iwai M, Shen JR (2008) Structures and functions of the extrinsic proteins of photosystem II from different species. Photosynth. Res. 98: 349-363

Ferreira KN, Iverson TM, Maghlaoui K, Iwata S, Barber J (2004) Architecture of the photosynthetic oxygen-evolving center. Science 303: 1831-1838

Gardian Z, Bumba L, Schrofel A, Herbstova M, Nebesarova J, Vacha F (2007) Organisation of Photosystem I and Photosystem II in red alga *Cyanidium caldarium*: encounter of cyanobacterial and higher plant concepts. Biochim. Biophys. Acta 1767: 725-731

Guskov A, Kern J, Gabdulkhakov A, Broser M, Zouni A, Saenger W (2009) Cyanobacterial photosystem II at 2.9-A resolution and the role of quinones, lipids, channels and chloride. Nat. Struct. Mol. Biol. 16: 334-342.

Kamiya N, Shen JR (2003) Crystal structure of oxygen-evolving photosystem II from *Thermosynechococcus vulcanus* at 3.7-A resolution. Proc. Natl Acad. Sci. 100: 98-103

Kargul J, Maghlaoui K, Murray JW, Deak Z, Vass I, Boussac A, Rutherford AW, Barber J (2007) Purification, crystallization and X-ray diffraction analyses of the *T. elongatus* PSII core dimer with strontium replacing calcium in the oxygen-evolving complex. Biochim. Biophys. Acta 1767: 404-413

Loll B, Kern J, Saenger W, Zouni A, Biesiadka J (2005) Towards complete cofactor arrangement in the 3.0 A resolution structure of photosystem II. Nature 438: 1040-1044

Murray JW, Maghlaoui K, Kargul J, Ishida N, Lai T-L, Rutherford AW, Sugiura M, Boussac A, Barber J (2008a) X-ray crystallography identifies two chloride binding sites in the oxygen evolving centre of Photosystem II. Energy Environ. Sci. 1: 161-166

Murray JW, Maghlaoui K, Kargul J, Sugiura M, Barber J (2008b) Analysis of Xenon binding to Photosystem II by X-ray crystallography. Photosynth. Res. 98: 523-527

Nowaczyk MM, Hebeler R, Schlodder E, Meyer HE, Warscheid B, Rögner M (2006) Psb27, a cyanobacterial lipoprotein, is involved in the repair cycle of photosystem II. Plant Cell 18: 3121-3131

Nozaki H, Matsuzaki M, Takahara M, Misumi O, Kuroiwa H, Hasegawa M, Shin-i T, Kohara Y, Ogasawara N, Kuroiwa T(2003) The phylogenetic position of red algae revealed by multiple nuclear genes from mitochondria-containing eukaryotes and an alternative hypothesis on the origin of plastids. J. Mol. Evol. 56: 485-497

Ohta H, Suzuki T, Ueno M, Okumura A, Yoshihara S, Shen J-R, Enami I (2003) Extrinsic proteins of photosystem II: an intermediate member of PsbQ protein family in red algal PSII. Eur. J. Biochem. 270: 4156-4163

Siegbahn PE (2009) Structures and energetics for O_2 formation in photosystem II. Acc Chem Res. 42: 1871-1880

Sproviero EM, Shinopoulos K, Gascón JA, McEvoy JP, Brudvig GW, Batista VS (2008) QM/MM computational studies of substrate water binding to the oxygen-evolving centre of photosystem II. Philos. Trans. R Soc. Lond. B Biol. Sci. 363: 1149-1156

Yano J, Kern J, Sauer K, Latimer MJ, Pushkar Y, Biesiadka J, Loll B, Saenger W, Messinger J, Zouni A, Yachandra VK. (2006) Where water is oxidized to dioxygen: structure of the photosynthetic Mn_4Ca cluster. Science 314: 821-825